Chemical Science

ROYAL SOCIETY OF CHEMISTRY

EDGE ARTICLE

View Article Online
View Journal | View Issue

Check for updates

Cite this: *Chem. Sci.*, 2025, **16**, 9863

All publication charges for this article have been paid for by the Royal Society of Chemistry

Received 20th September 2024
Accepted 12th April 2025

DOI: 10.1039/d4sc06391k

rsc.li/chemical-science

Potassium *tert*-butoxide mediated stereoselective/direct Mannich reaction of α-substituted-γ-lactams with *in situ* generated aryl *N*-silyl imines†

Tyler D. Casselman,[a] Mithun C. Madhusudhanan,[b] Binh Khanh Mai,[b] Peng Liu ‡[b] and Brian M. Stoltz ‡[a]

A potassium *tert*-butoxide (KO*t*-Bu)-mediated Mannich reaction between α-substituted-γ-lactams and *N*-silyl imines is reported. *N*-silyl imines are generated *in situ* from readily available aryl nitriles and directly combined with the lactams, without preformation of the lactam enolate, to afford the α-quaternary center-bearing Mannich bases in high yield and with high diastereoselectivity (24 examples). This reaction is shown to be catalytic with respect to KO*t*-Bu and the catalytic mechanism has been investigated using density functional theory calculations. The computational investigations suggest that the diastereoselectivity is controlled by explicit interactions between a binuclear potassium complex and both the imine nitrogen and the enolate oxygen atoms in the selectivity-determining transition states. The Mannich products are shown to be useful in accessing novel spirocyclic pyrrolidines.

Introduction

Since the seminal report in 1912[1] the Mannich reaction has become an important method for C–C bond formation in synthetic organic chemistry.[2] The resulting β-amino carbonyl motif produced by this reaction is present in many alkaloid natural products[3] and biologically relevant molecules.[4] Due to its synthetic utility, the Mannich reaction has received significant attention since the early 1990's,[5] particularly toward the development of stereoselective variants.[6] Despite the prevalence of quaternary centers in complex synthetic targets,[7] the stereoselective Mannich reactions using non-stabilized enolates forming such quaternary centers remains largely underexplored.[8] A significant number of these reports rely on the enolate-stabilization (pK_a < 30 in DMSO)[9] provided by an α-electron-withdrawing[10] or an α-aryl[11] group to achieve *in situ* enolization and the desired reactivity. Notable exceptions include those reported by the Barbas group[12] and the Trost group,[13] utilizing α-substituted aldehydes and ketones. To our knowledge, a stereoselective Mannich reaction using unstabilized, α-substituted lactams as pro-nucleophiles to form quaternary centers has not been reported.

Using amides as pro-nucleophiles has been a significant challenge in developing stereoselective Mannich reactions due to their low C–H acidity ($pK_a \approx 30$–35 in DMSO)[9] and the instability of the corresponding metal enolates.[14] To overcome these challenges, amide auxiliaries have been critical to promote these stereoselective Mannich reactions (Scheme 1a).[15] These auxiliaries have proven to be effective; however, they require additional steps for installation and removal, and are incompatible with cyclic, lactam pro-nucleophiles. A few notable examples using simple, amide pro-nucleophiles without the need for auxiliaries were reported by the Yamaguchi group[16] in 2010 and, more recently, the Kobayashi group in 2021.[17] To circumvent the isolation of the unstable amide enolates, the Yamaguchi group[16] developed a catalytic soft enolization to promote the diastereoselective direct Mannich reaction (Scheme 1b). Similarly, the Kobayashi group[17] worked to address enolate stability by designing a chiral potassium salt catalyst to deliver enantioenriched Mannich bases with simple, acyclic amide pro-nucleophiles (Scheme 1c). However, these systems have not been demonstrated to promote the stereoselective, direct Mannich reaction using α-substituted, unactivated amides to generate quaternary centers. Here we report a protocol that enables the diastereoselective direct Mannich reaction of simple, α-branched unactivated γ-lactams in high diastereoselectivity.[18] To the best of our knowledge, this is the first report on the utilization of simple, α-substituted amide pro-nucleophiles in a diastereoselective direct Mannich reaction without preformation of the lactam enolate.

[a]*Warren and Katherine Schlinger Laboratory for Chemistry and Chemical Engineering, Division of Chemistry and Chemical Engineering, California Institute of Technology, 1200 East California Boulevard, Pasadena, CA 91125, USA. E-mail: stoltz@caltech.edu*

[b]*Department of Chemistry, University of Pittsburgh, 4200 Fifth Avenue, Pittsburgh, PA 15260, USA*

† Electronic supplementary information (ESI) available: Experimental procedures, spectroscopic data (^{1}H NMR, ^{13}C NMR, IR, HRMS), computational details, Cartesian coordinates, and energies of DFT-computed structures. CCDC 2253010, 2253012 and 2253013. For ESI and crystallographic data in CIF or other electronic format see DOI: https://doi.org/10.1039/d4sc06391k

‡ Principal Investigator

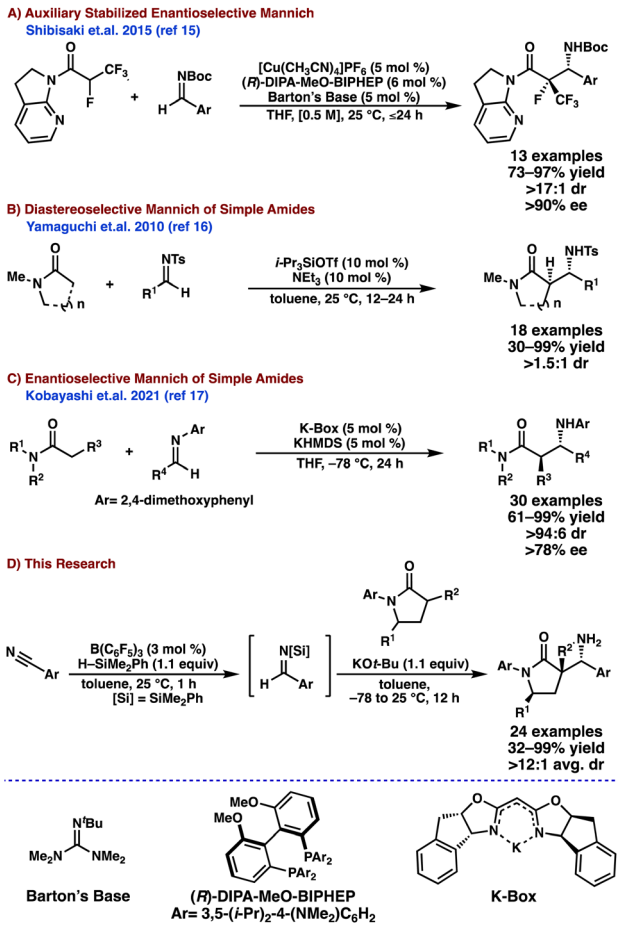

Scheme 1 Stereoselective Mannich reaction of Amides.

Results and discussion

We began investigating the use of unactivated α-substituted-γ-lactam **1** as a Mannich donor with *N*-acyl imine **3a** as the acceptor and employing LiHMDS as the base. We discovered that the unactivated lactam **1** is a competent pro-nucleophile under these conditions, but the diastereoselectivity and yield of the reaction were low (Table 1, entry 1). Increasing the temperature to 25 °C led to increased yield, but the dr remained low (Table 1, entry 2). Changing the acceptor from the *N*-acyl imine **3a** to the *N*-silyl imine **3b** resulted in the desired C–C bond formation in moderate yield, but an unexpected imine condensation adduct **5** was observed and isolated along with the desired Mannich base **4** (Table 1, entry 3). Using KO*t*-Bu as the base drastically improved the overall yield and minimized the formation of **5**. The lability of the N–Si bond allowed for the primary amine **4** to be isolated in 85% yield and a 9 : 1 dr after aqueous workup (Table 1, entry 5). Finally, switching from the *ortho*-methoxy-phenyl (OMP) lactam **1** to the *para*-methoxy-phenyl (PMP) lactam **2** dramatically improved the dr to 20 : 1 and increased the yield to 90% (Table 1, entry 6). Using these conditions, the reaction can be performed on a 1 mmol scale with similar yield and dr (Table 1, entry 7). Having identified the optimized reaction conditions, we next turned to exploring the

Table 1 Optimization of the Mannich reaction[a]

Entry	Base	Imine	T (°C)	R^1 [c]	4[d] (dr)	5[d]
1	LiHMDS	**3a**	−10 °C	Bz	20% (2 : 1)	0%
2	LiHMDS	**3a**	25 °C	Bz	40% (2 : 1)	0%
3	LiHMDS	**3b**	−10 °C	H(TMS)	20% (2 : 1)	40%
4	LiHMDS	**3b**	−40 °C	H(TMS)	14% (2 : 1)	36%
5	KO*t*-Bu	**3b**	−40 °C	H(TMS)	85% (9 : 1)	5%
6[b]	KO*t*-Bu	**3b**	−40 °C	H(TMS)	90% (20 : 1)	5%
7[b,e]	KO*t*-Bu	**3b**	−40 °C	H(TMS)	95% (20 : 1)	0%

[a] Reaction conditions: **1** (0.2 mmol), **3** (1.0 equiv.), 3.0 mL toluene at X ° C, 8 h; [b] Lactam **2** was used instead of **1**. [c] When imine **3b** is used, product **4** was observed as the primary amine. [d] Isolated yields. [e] Reaction was performed with 1.0 mmol **2**, 1.5 equiv. **3b**, 15.0 mL toluene, −40 to 25 °C, 8 h. *ortho*-OMe-Ph (OMP), *para*-OMe-Ph (PMP).

generality of the reaction with respect to the α-substitution of the lactam.

Gratifyingly, the reaction tolerates larger alkyl substituents, as lactams **2a–c** afforded the desired Mannich products **4a–c** (Scheme 2) as the primary amine in high yields and diastereomeric ratios. To our delight, performing the reaction using lactam **2a** on a 1 mmol scale delivered the corresponding product **4a** in 87% yield and a 20 : 1 dr. A major limitation to the scope of our reaction was the need to isolate the water-sensitive *N*-silyl imine **3b**. Our initial approach toward synthesizing the *N*-silyl imine was through an Aza-Peterson reaction to afford imine **3b**.[19] Due to the instability of *N*-silyl imines and challenging isolation,[20] we focused our efforts to develop a telescoped hydrosilylation/direct Mannich process.

We began our investigation of a telescoped process with a modified catalytic hydrosilylation procedure using H–SiMe$_2$Ph and catalytic B(C$_6$F$_5$)$_3$ in toluene (Scheme 3).[21] Following the catalytic hydrosilylation, the reaction mixture was directly added to a solution of KO*t*-Bu and lactam **2** in toluene to perform the diastereoselective Mannich reaction.

A variety of Mannich donor substrates possessing α-alkyl substitution were subjected to this telescoped reaction

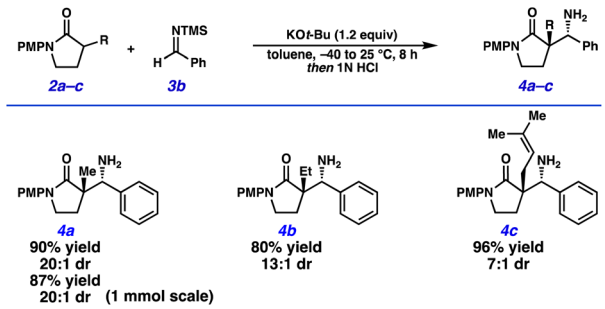

Scheme 2 Preliminary scope of α-substituted lactams.

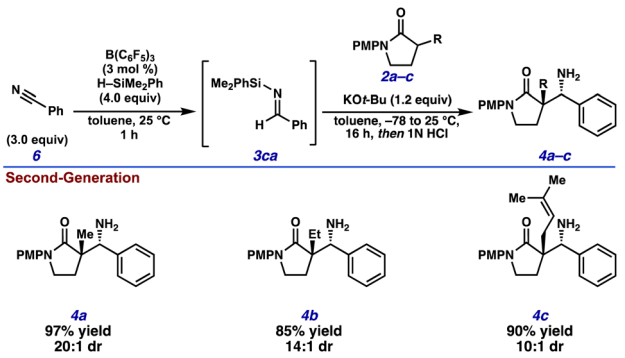

Scheme 3 Alternative synthesis of *N*-silyl imines.

sequence (Scheme 4). An excess of the aryl nitrile **6** was shown to be necessary for complete conversion of the lactam Mannich donor due to the formation of the imine transfer adduct between the silyl imine Mannich acceptor **3ca** and the Mannich base **4**, resulting in products akin to **5**. Gratifyingly, this side product can be hydrolyzed upon workup to afford the primary amine **4**. Notably, *in situ* generated imine **3ca** (Scheme 3) performed comparably using the telescoped catalytic conditions to those obtained through the two step Aza-Peterson approach. The use of excess aryl nitrile for electron deficient substrates (Scheme 4) was necessary to generate a sufficient concentration of the desired imine as overreduction to the benzyl amine catalysed by $B(C_6F_5)_3$ was observed in the crude reaction mixture after hydrosilylation.

Allylic and benzylic substitution was generally tolerated at the α-position of the γ-lactam pro-nucleophile (Scheme 4). Gratifyingly, we observed the reaction performed well on modest scale as product **4d** was isolated in an 86% yield and 14 : 1 dr. Sterically congested motifs such as the *ortho*-Br and *ortho*-CN benzylic lactams (**4f** and **4g**) gave the desired products in moderate yield and diastereoselectivity, requiring ethereal cosolvents to assist in solubility of the bulkier lactam pro-nucleophiles. Mannich donors bearing β-tertiary carbon centers were also competent, delivering the desired products **4h** and **4i** in good diastereoselectivity. Notably, β-amino lactam **4i** possesses three contiguous stereocenters formed with a 9 : 1 ratio of the major diastereomer relative to all others, potentially owing to $A_{1,3}$ strain in the corresponding potassium enolate of **2i**.[22] Lactam donor **2j**, possessing a methyl group at the γ-position, afforded the desired Mannich product **4j** in 95% yield and 10 : 1 dr (see ESI† for details on the tentative assignment of the relative stereochemistry of **4i** and **4j**).[22] This suggests that substitution on the backbone of the γ-lactam can impart facial selectivity for the approach of the *N*-silyl imine electrophile. For the electrophile scope, electron-neutral as well as electron-deficient arenes are well tolerated in the telescoped reaction sequence. Electron-releasing substituents on the aryl nitrile were not viable pro-electrophiles for the transformation due to the inability to engage in the $B(C_6F_5)_3$-catalyzed hydrosilylation under our optimized reaction conditions.[23] Additionally, we observed the rate of hydrosilylation and the susceptibility of the *N*-silyl imines to undergo exhaustive hydrosilylation to the corresponding benzylic amine to be dependent on the substitution of the aryl nitrile. *Ortho*-substitution on the aryl nitriles delivered the desired amines **4l**, **4o**, and **4u** bearing a trifluoromethyl, fluoro and bromo group respectively.

Notably, the more sterically demanding[24] and electron withdrawing[25] *ortho*-CF_3 group afforded the Mannich base **4l** in an excellent 20 : 1 dr, while the *ortho*-F substituted aryl nitrile

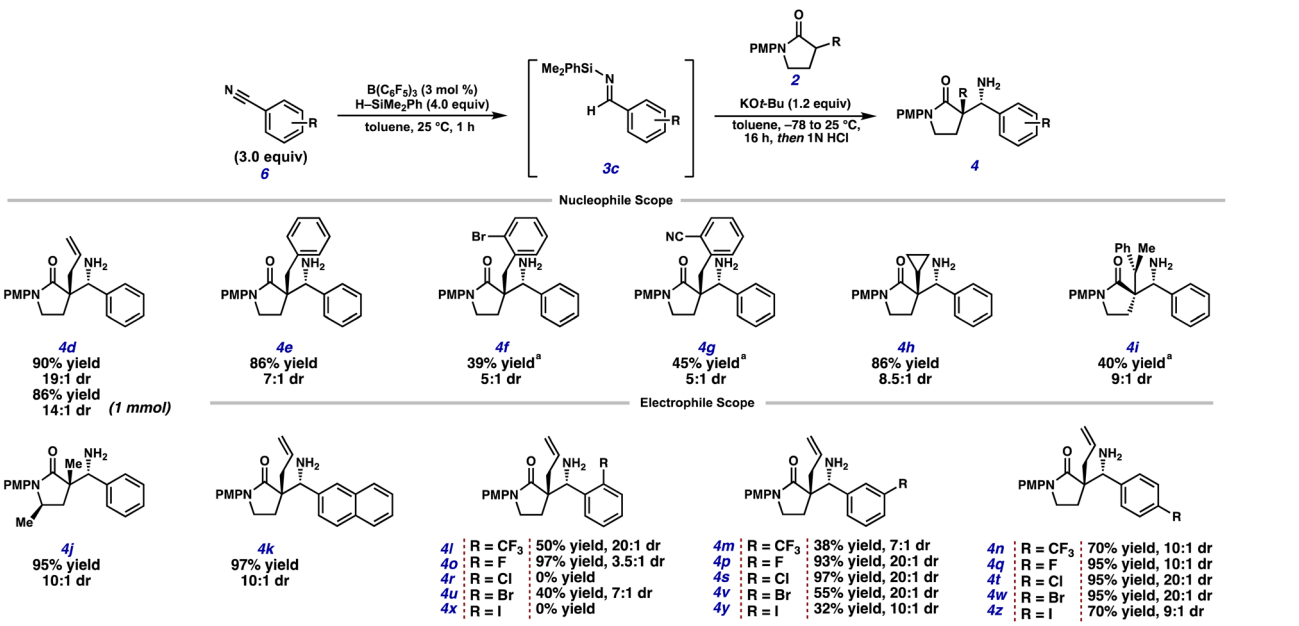

Scheme 4 Substrate scope for the tandem hydrosilylation/direct Mannich reaction. Standard reaction conditions: 1st step: **6** (3.0 equiv.), $B(C_6F_5)_3$ (3 mol%), $PhMe_2SiH$ (4.0 equiv.), toluene (1 mL), 25 °C, 1 h; 2nd step: **2** (0.2 mmol), KOt-Bu (1.2 equiv.), toluene (2 mL), −78 to 25 °C, 16 h (a) Et_2O (0.5 mL) was added in the 2nd step.

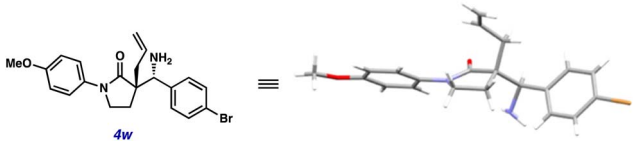

Fig. 1 Xray structure of **4w**. For the detailed procedure and conditions, see ESI.† CCDC 2253010.

delivered the product **4o** in a modest 3.5 : 1 dr. Unfortunately, the *ortho*-Cl and *ortho*-I substituted aryl nitriles (**4r** and **4x**) did not deliver any desired product due to failures at the hydrosilylation portion of the tandem sequence.[26] Gratifyingly, *meta*- and *para*-substitution on the arene was well tolerated for electron withdrawing substituents, as the corresponding products were obtained in modest to excellent yield with high diastereoselectivity. The relative stereochemistry was unambiguously confirmed by X-ray diffraction (Fig. 1). By analogy, the relative configuration was adopted for the remaining scope entries.

The primary amine products provide an excellent functional group handle to allow for further derivatization *via* *N*-functionalization and cross-coupling chemistry. Primary amine **4d** underwent facile *N*-Ts and *N*-Boc protection to afford the corresponding protected amines **7** and **8** in 96% and 95% yields, respectively. Protected amines **7** and **8** cleanly underwent a CAN-promoted *N*-PMP cleavage to afford the secondary amides **9** and **10**, respectively, in excellent yields (Scheme 5).

Functionalization of β-amino lactam **4d** with acryloyl chloride delivered acrylamide **12** in an 88% yield (Scheme 6). Subjecting acrylamide **12** to Grubbs' 2nd generation catalyst led to the isolation of the desired spirocyclic ε-lactam **13** in 84% yield.[27] Inspired by Wolfe's two-step, one-pot intramolecular carboamination, we subjected amine **4d** to the disclosed Pd-catalyzed conditions.[28] Gratifyingly, the reaction proceeds with an 82% yield for the bis-arylated spirocyclic pyrrolidine **15a** using bromobenzene as the aryl halide electrophile without the need to isolate the intermediate aniline **14a**. Using the more electron-rich 4-bromoanisole led to lower yield and diastereoselectivity of the isolated spirocyclic product **15b** with significant isolation of the retro-Mannich product **2d**.

Gratifyingly, using 3,5-dimethyl bromobenzene as the aryl halide delivered the desired spirocyclic pyrrolidine **15c** in good yield and diastereoselectivity. Highly electron-deficient aryl halides such as 3-bromopyridine were not tolerated. Additionally, using the *N*-Boc protected product **8** as a substrate for the Pd-catalyzed carboamination led to the formation of the *N*-Boc pyrrolidine **16** using electron-rich aryl halides. However,

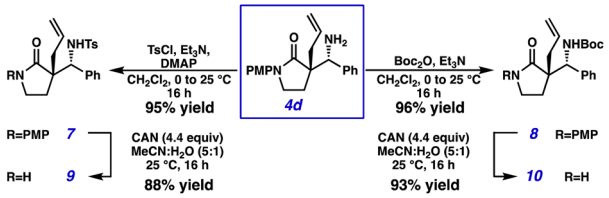

Scheme 5 Protecting group manipulation of Mannich product **4d**.

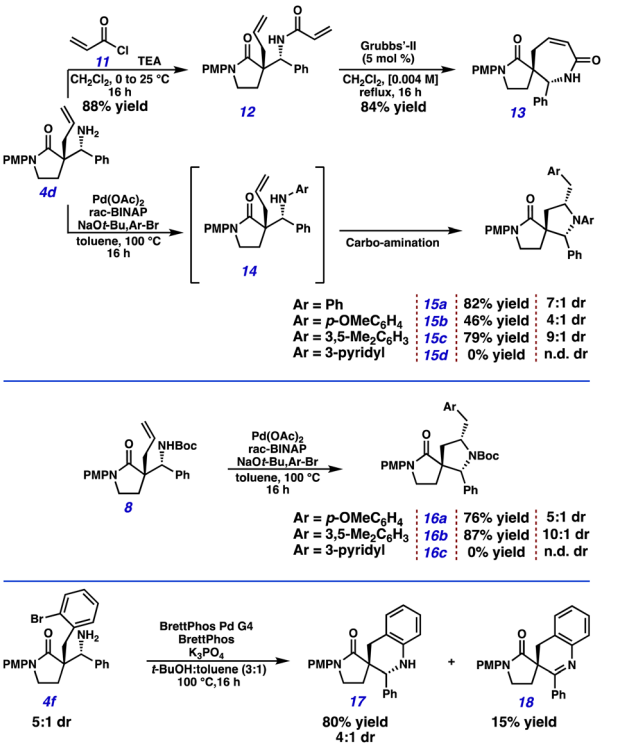

Scheme 6 Selected spirocyclizations of Mannich products.

electron-deficient aryl halides such as 3-bromopyridine were not tolerated. We also identified *ortho*-Br benzylic product **4f** as a suitable candidate for an intramolecular Buchwald–Hartwig-type coupling.[29] Subjecting amine **4f** to the intramolecular C–N arylation afforded spirocyclic tetrahydroquinoline **17** in an 80% yield, but diminished diastereoselectivity. A minor product **18** assigned as the dihydroquinoline was observed, presumably arising from the oxidation of the major *anti* diastereomer resulting in lower dr of the isolated tetrahydroquinoline **17**.[30]

During our optimization campaign, we discovered that substoichiometric KO*t*-Bu can be employed while still delivering the resulting Mannich product in up to 95% yield and 12 : 1 dr with base loadings as low as 35 mol% (see Scheme S3† for details).[31] As shown in Scheme 7, we hypothesized that formation of potassium enolate **2a′** through the deprotonation of lactam **2a** with KO*t*-Bu dimer **19b** would liberate an equivalent of *tert*-butanol, which could serve to protonate potassium amide **20** formed after C–C bond formation and regenerate the KO*t*-Bu dimer **19b** (Scheme 7).[32] The *N*-silyl amine product **21** would then be protonated upon aqueous work up to deliver the desired product **4a**.

The mechanism that controls the diastereoselectivity of the Mannich reaction and the potential role of KO*t*-Bu[17,32] was investigated using density functional theory (DFT) calculations.[33,34] Considering the potassium *tert*-butoxide tetramer can easily dissociate to a dimer,[32a] and binuclear potassium complexes[32,35] have been described in previous reports as the active species in the potassium-catalyzed α-alkylation of benzyl sulfides,[36] dimeric potassium *tert*-butoxide was used as the base in the calculations, in which one toluene solvent molecule was

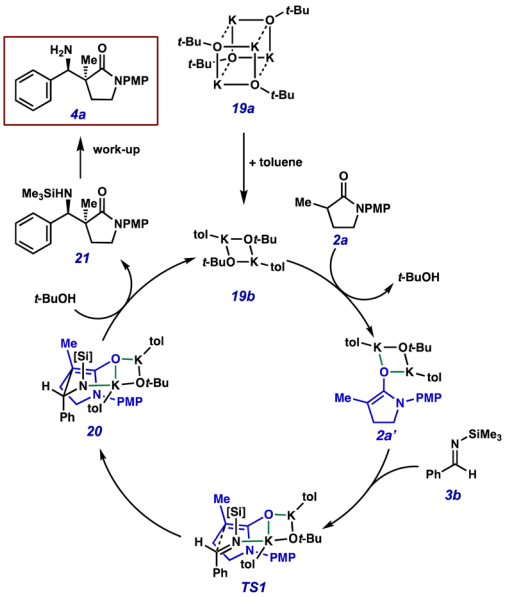

Scheme 7 Proposed catalytic cycle.

added to bind to each potassium to account for explicit solvent effects. Our DFT calculations indicate that deprotonation of lactam **2a** with potassium *tert*-butoxide dimer to form potassium enolate **2a′** is endergonic by 2.3 kcal mol^{-1} (see Fig. S3†). After careful conformational search of the transition state (TS) of the reaction between **2a′** and imine **3b**, we located the lowest-energy TS conformers, **TS1** and **TS2**, leading to the *anti*- and *syn*-products **4a** and **4a-epi**, respectively (Fig. 2 and S5 in the ESI† for the computed reaction energy profiles). The computed activation free energy for **TS1** ($\Delta G^{\ddagger}$ = 14.2 kcal mol^{-1} with respect to **2a**) is 2.3 kcal mol^{-1} lower than that for **TS2** ($\Delta G^{\ddagger}$ = 16.5 kcal mol^{-1}), which is in agreement with the experimentally observed diastereoselectivity of 20 : 1. In **TS1** and **TS2**, both potassium atoms bind to the *tert*-butoxide oxygen and the enolate oxygen, forming a rhombus-shaped geometry that resembles the KO*t*-Bu dimer. Although this four-atom K_2O_2 core structure remains similar in **TS1** and **TS2**, when the different prochiral π-faces of the imine are involved in bond formation, different interactions between the imine and potassium are observed.

In the transition state leading to the favoured anti-product (**TS1**), the imine C=N bond is synclinal with the enolate oxygen, enabling a stabilizing interaction (2.69 Å) between the electron-rich imine nitrogen and one of the potassium atoms. The relatively late transition state, evidenced by the shorter forming C–C bond (2.08 Å compared to 2.23 Å in **TS2**), increases the negative charge on the imine nitrogen (see Fig. S4† for computed NPA charges) and thus further promotes the N–K interaction in **TS1**. In **TS2**, the Ph group on the imine, rather than imine C=N bond, points towards the enolate oxygen and the potassium atoms.

As a result, a cation–π interaction[37] (2.95 Å) between a potassium and the Ph group is observed, in place of the N–K interaction. Because the Ph group is less negatively charged and is a worse donor than the imine nitrogen, this cation–π interaction is expected to be weaker than the N–K interaction in **TS1**.

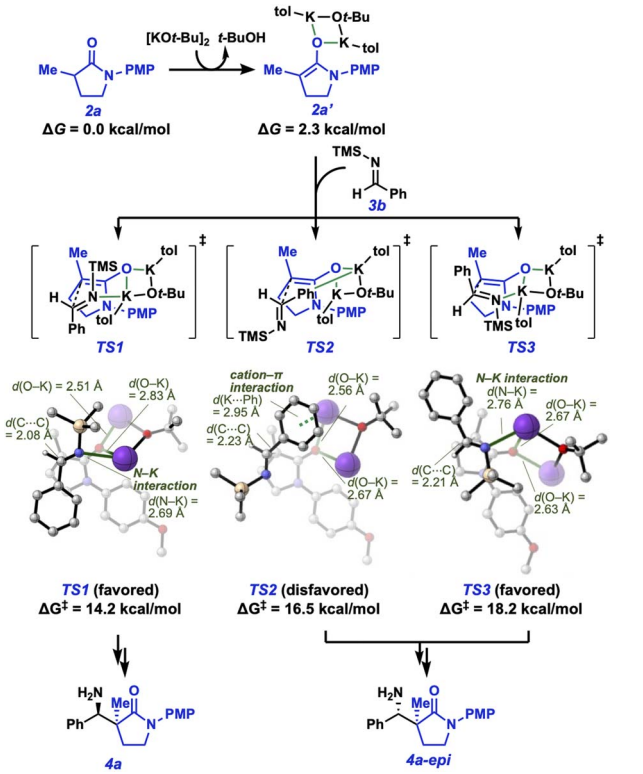

Fig. 2 Computed imine addition pathways involving a dipotassium enolate complex **2a′**. Gibbs free energies are calculated with respect to lactam **2a**, [KO*t*-Bu]$_2$, and imine **3b**. Toluene molecules in the 3D images are omitted for clarity.

The imine N–K interaction was also observed in a less stable TS conformer (**TS3**) leading to the minor product **4a-epi**. **TS3** is less stable than both **TS1** and **TS2** because this stereoisomeric transition state has a boat geometry rather than the chair geometry in **TS1** and **TS2**. Taken together, the DFT calculations indicate that the stabilizing imine–potassium interaction in the chair-like imine addition transition state (**TS1**) controls the diastereoselectivity of the Mannich reaction.

We took inspiration from the Kobayashi report[17] to render this transformation asymmetric *via* introduction of a catalytic, chiral potassium salt. Catalytic levels of KO*t*-Bu were required to suppress the racemic, background Mannich reaction. Gratifyingly, we observed modest levels of stereoselectivity with the introduction of **K-Box-1**, delivering the desired amine **4b** in 60% ee with good yield and dr (Table 2, entry 1).

Utilizing Indabox precatalyst **L2** lacking the acidic methylene C–H bond in precatalyst **L1** resulted in suppression of reactivity and stereoselectivity, suggesting that the potassium salt is the active catalyst in this transformation. Significant optimization of solvent and stoichiometry (see Table S2†) resulted in no improvement of the observed enantioselectivity. To improve the enantioselectivity of this transformation, we focused on altering the silane identity to provide a handle to modify the steric and electronic influence around the imine electrophile. Diaryl silanes required elevated temperatures to perform the hydrosilylation (Table 2, entries 3–4); however, the telescoped

Table 2 Optimization of the asymmetric Mannich reaction[a]

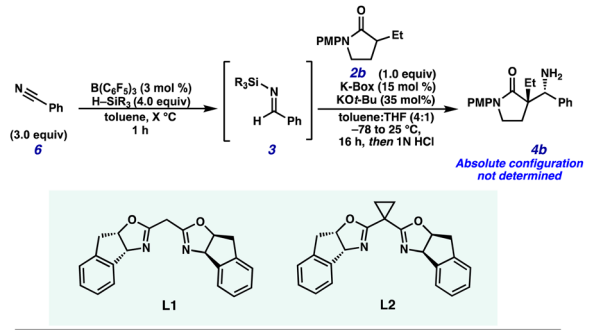

Entry	H-SiR$_3$	X (°C)	**4b** (dr)	% ee
1	$PhMe_2SiH$	25 °C	93% (12 : 1)	60%
2	$PhMe_2SiH$[b]	25 °C	33% (11 : 1)	3%
3	Ph_2MeSIH	40 °C	95% (10 : 1)	4%
4	Ph_2SiH_2	40 °C	85% (11 : 1)	3%
5	Ph_3SiH[c]	100 °C	0% (n.d.)	n.d
6	*t*-$BuMe_2SiH$[c]	40 °C	0% (n.d.)	n.d
7	Et_3SiH	25 °C	17% (11 : 1)	52%
8	$BnMe_2SiH$	25 °C	89% (13 : 1)	72%

[a] **K-Box**: Dissolve **L1** (15 mol%) and KHMDS (15 mol%) in THF (0.75 mL) at 0 °C for 0.5 h **Imine 3**: nitrile **6** (0.6 mmol), $B(C_6F_5)_3$, silane (0.8 mmol) in toluene at X °C. **4b**: Add **K-Box** to a solution of **2b** (0.2 mmol) in toluene (3.0 mL) at −78 °C, add **Imine 3** slowly and held at 25 °C overnight. [b] **L2** was used instead of **L1**. [c] No hydrosilylation observed.

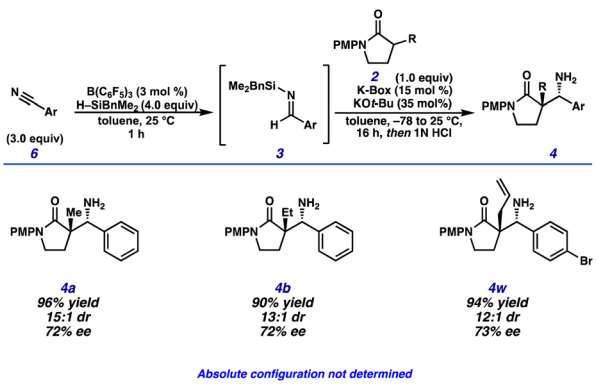

Scheme 8 Preliminary substrate scope for the enantioselective transformation.

Mannich reaction proceeded in much lower levels of enantioselectivity. Electronically deficient Ph_3Si–H and sterically bulky *t*-$BuMe_2Si$–H were unable to perform the hydrosilylation, even at elevated temperatures (Table 2, entries 5–6). Triethyl silane promoted the desired telescoped hydrosilylation/Mannich reaction, but in diminished yield and enantioselectivity. Gratifyingly, performing the telescoped process using $BnMe_2Si$–H resulted in the formation of amine **4b** in good yield, dr, and an improved enantioselectivity of 72% ee (Table 2, entry 8). Additional optimization of the silane source resulted in no further improvement to date (see Scheme S4†).

After extensive optimization of the reaction conditions, we focused our efforts toward determining if the observed enantioselectivity was general to other aryl nitrile pro-electrophiles and lactam pro-nucleophiles. To our delight, Mannich products **4a**, **4b** and **4w** were synthesized in great yield and diastereoselectivity while maintaining a modest enantioselectivity (72–73% ee) (Scheme 8). Further investigation is ongoing to identify the absolute configuration of the products formed, improve the enantioselectivity and scope of this telescoped transformation.

Conclusion

In conclusion, we have reported a telescoped hydrosilylation/direct Mannich reaction that couples α-substituted-γ-lactams with aryl nitriles to afford β-amino lactam products bearing an all-carbon quaternary stereocenter. This two-step, one-pot process generates the desired Mannich bases in excellent diastereoselectivity and yield. Electron-neutral and electron-poor aryl nitriles were demonstrated to be competent pro-electrophiles, and a wide α-substitution scope of the pro-nucleophiles has been established. The Mannich products have been shown to be valuable building blocks for further exploration, especially toward the synthesis of complex spirocyclic saturated N-heterocycles. The reaction was shown to be promoted by substoichiometric levels of KOt-Bu, as low as 35 mol%, with computational analysis elucidating a potential mechanism for catalysis as well as the transition states involving a binuclear potassium complex promoting the desired C–C bond formation and controlling the diastereoselectivity. Further investigations toward rendering this transformation asymmetric are ongoing in our laboratory and will be disclosed in due course.

Data availability

The data supporting this article have been included as part of the ESI.†

Author contributions

Conceptualization: T. D. C. and B. M. S. Experimental methodology: T. D. C. and B. M. S. Computational methodology: M. C. M., B. K. M., and P. L. Funding acquisition: B. M. S. and P. L. Project administration: B. M. S. and P. L. Supervision: B. M. S. and P. L. Writing – original draft: T. D. C. Writing – review and editing: T. D. C., M. C. M., B. K. M., P. L. and B. M. S.

Conflicts of interest

There are no conflicts to declare.

Acknowledgements

The authors thank Dr Scott Virgil and Alex Cusumano for helpful discussions, David VanderVelde for NMR assistance, Dr Michael Takase for XRD assistance, and Dr Mona Shahgholi for mass spectrometry assistance. The authors thank the Beckman

Institute for their support of the Caltech XRD facility, as well as the Dow Next Generation Instrument Grant. The authors (BMS and TDC) thank NIH (R35GM145239) and the Heritage Medical Research Institute Investigator Program. Further financial support for this work was provided by NSF (CHE-2247505 to P. L.). Computational studies were performed at the Center for Research Computing at the University of Pittsburgh and the Advanced Cyberinfrastructure Coordination Ecosystem: Services & Support (ACCESS) program supported by NSF. Constructive discussions within the Catalysis Innovation Consortium facilitated this collaborative study.

Notes and references

1 C. Mannich and W. Krösche, *Arch. Pharm.*, 1912, **250**, 647–667.

2 For a recent review on the asymmetric Mannich reaction, see: (*a*) S. Kobayashi, Y. Mori, J. S. Fossey and M. M. Salter, *Chem. Rev.*, 2011, **111**, 2626–2704. For a review on advances in Metal-catalyzed asymmetric Mannich reactions, see: (*b*) B. E. Karimi Dieter and E. Jafari, *Synthesis*, 2013, **45**, 2769–2812. For a review on bimetallic Mannich reactions, see: (*c*) M. Shibasaki, M. Kanai, S. Matsunaga and N. Kumagai, *Acc. Chem. Res.*, 2009, **42**, 1117–1127. For a microreview on the organocatalytic Mannich reaction, see: (*d*) A. Ting and S. E. Schaus, *Eur. J. Org Chem.*, 2007, **2007**, 5797–5815. For a review on the direct catalytic Mannich reaction, see: (*e*) A. Córdova, *Acc. Chem. Res.*, 2004, **37**, 102–112.

3 For a recent review on the use of intramolecular Mannich reactions toward the synthesis of natural products, see: (*a*) Y. Shi, Q. Wang and S. Gao, *Org. Chem. Front.*, 2018, **5**, 1049–1066. For select examples of intermolecular asymmetric Mannich-type reactions used in the synthesis of natural products, see: (*b*) Y. Numajiri, B. P. Pritchett, K. Chiyoda and B. M. Stoltz, *J. Am. Chem. Soc.*, 2015, **137**, 1040–1043; (*c*) M. Cushman and J. K. Chen, *J. Org. Chem.*, 1987, **52**, 1517–1521; (*d*) B. M. Trost, C.-I. J. Hung and Z. Jiao, *J. Am. Chem. Soc.*, 2019, **141**, 16085–16092; (*e*) A. E. Cholewczynski, P. C. Williams and J. G. Pierce, *Org. Lett.*, 2020, **22**, 714–717.

4 For a review on the use of Mannich reactions in medicinal chemistry and drug design, see: G. Roman, *Eur. J. Med. Chem.*, 2015, **89**, 743–816.

5 For a mini review on the history of the Mannich reaction in the 1990's, see: S. Kobayashi and H. Ishitani, *Chem. Rev.*, 1999, **99**, 1069–1094.

6 For the first examples of an asymmetric Mannich reaction, see: (*a*) E. J. Corey, C. P. Decicco and R. C. Newbold, *Tetrahedron Lett.*, 1991, **32**, 5287–5290; (*b*) K. Ishihara, M. Miyata, K. Hattori, T. Tada and H. Yamamoto, *J. Am. Chem. Soc.*, 1994, **116**, 10520–10524; (*c*) H. Ishitani, M. Ueno and S. Kobayashi, *J. Am. Chem. Soc.*, 1997, **119**, 7153–7154; (*d*) S. Kobayashi, H. Ishitani and M. Ueno, *J. Am. Chem. Soc.*, 1998, **120**, 431–432; (*e*) S. Kobayashi, J. Kobayashi, H. Ishiani and M. Ueno, *Chem. - Eur. J.*, 2002, **8**, 4185–4190; (*f*) S. Yamasaki, T. Iida and M. Shibasaki, *Tetrahedron*, 1999, **55**, 8857–8867; (*g*) B. List, P. Pojarliev, W. T. Biller and H. J. Martin, *J. Am. Chem. Soc.*, 2002, **124**, 827–833.

7 For reviews on the construction of all-carbon quaternary centers and their significance in natural products, see: (*a*) J. Christoffers and A. Mann, *Angew. Chem., Int. Ed.*, 2001, **40**, 4591–4597; (*b*) C. J. Douglas and L. E. Overman, *Proc. Natl. Acad. Sci. U. S. A.*, 2004, **101**, 5363–5367; (*c*) T. Ling and F. Rivas, *Tetrahedron*, 2016, **72**, 6729–6777; (*d*) Z. Xin, H. Wang, H. He and S. Gao, *Tetrahedron Lett.*, 2021, **71**, 153029; (*e*) E. V. Prusov, *Angew. Chem., Int. Ed.*, 2017, **56**, 14356–14358; (*f*) C. Li, S. S. Ragab, G. Liu and W. Tang, *Nat. Prod. Rep.*, 2020, **37**, 276–292.

8 For an example of an asymmetric Mannich reaction using an α-substituted lactone pro-nucleophile, see: (*a*) M. Shang, M. Cao, Q. Wang and M. Wasa, *Angew. Chem., Int. Ed.*, 2017, **56**, 13338–13341. For a stereoselective Mannich reaction using a carboxylic acid pro-nucleophile, see: (*b*) Y. Morita, T. Yamamoto, H. Nagai, Y. Shimizu and M. Kanai, *J. Am. Chem. Soc.*, 2015, **137**, 7075–7078.

9 F. G. Bordwell, *Acc. Chem. Res.*, 1988, **21**, 456–463.

10 For selected examples of malonate-type Mannich donors, see: (*a*) M. Hatano, T. Horibe and K. Ishihara, *J. Am. Chem. Soc.*, 2010, **132**, 56–57; (*b*) T. Poisson, T. Tsubogo, Y. Yamashita and S. Kobayashi, *J. Org. Chem.*, 2010, **75**, 963–965; (*c*) Y. K. Kang and D. Y. Kim, *J. Org. Chem.*, 2009, **74**, 5734–5737; (*d*) T. Kano, C. Homma and K. Maruoka, *Org. Biomol. Chem.*, 2017, **15**, 4527–4530; (*e*) T. Kano, T. Yurino and K. Maruoka, *Angew. Chem., Int. Ed.*, 2013, **52**, 11509–11512; (*f*) S. Lou, P. Dai and S. E. Schaus, *J. Org. Chem.*, 2007, **72**, 9998–10008; (*g*) Y.-P. Lou, C.-W. Zheng, R.-M. Pan, Q.-W. Jin, G. Zhao and Z. Li, *Org. Lett.*, 2015, **17**, 688–691; (*h*) J. H. Lee and D. Y. Kim, *Adv. Synth. Catal.*, 2009, **351**, 1779–1782; (*i*) R. Pan, J. Zhang, C. Zheng, H. Wang, D. Cao, W. Cao and G. Zhao, *Tetrahedron*, 2017, **73**, 2349–2358; (*j*) Q. Guo and J. C.-G. Zhao, *Org. Lett.*, 2013, **15**, 508–511; (*k*) X. Jiang, D. Fu, G. Zhang, Y. Cao, L. Liu, J. Song and R. Wang, *Chem. Commun.*, 2010, **46**, 4294–4296.

11 For selected examples of indalone Mannich donors, see: (*a*) S. Shimizu, T. Tsubogo, P. Xu and S. Kobayashi, *Org. Lett.*, 2015, **17**, 2006–2009; (*b*) R. He, C. Ding and K. Maruoka, *Angew. Chem., Int. Ed.*, 2009, **48**, 4559–4561; (*c*) X. Tian, K. Jiang, J. Peng, W. Du and Y.-C. Chen, *Org. Lett.*, 2008, **10**, 3583–3586; (*d*) L. Cheng, L. Liu, H. Jia, D. Wang and Y.-J. Chen, *J. Org. Chem.*, 2009, **74**, 4650–4653; (*e*) Q. Jin, C. Zheng, G. Zhao and G. Zou, *Tetrahedron*, 2018, **74**, 4134–4144; (*f*) M. Torii, K. Kato, D. Uraguchi and T. Ooi, *Beilstein J. Org. Chem.*, 2016, **12**, 2099–2103.

12 N. S. Chowdari, J. T. Suri and C. F. Barbas, *Org. Lett.*, 2004, **6**, 2507–2510.

13 For selected examples, see: (*a*) B. M. Trost, T. Saget and C.-I. (Joey) Hung, *J. Am. Chem. Soc.*, 2016, **138**, 3659–3662; (*b*) B. M. Trost, C.-I. J. Hung and E. Gnanamani, *ACS Catal.*, 2019, **9**, 1549–1557; (*c*) B. M. Trost and C.-I. (Joey) Hung, *J. Am. Chem. Soc.*, 2015, **137**, 15940–15946; (*d*) B. M. Trost, C.-I. J. Hung, G. Mata, Y. Liu, Y. Lu and E. Gnanamani, *Org. Lett.*, 2020, **22**, 2437–2441; (*e*)

B. M. Trost, T. Saget, A. Lerchen and C.-I. (Joey) Hung, *Angew. Chem., Int. Ed.*, 2016, **55**, 781–784; (*f*) B. M. Trost, T. Saget and C.-I. (Joey) Hung, *Angew. Chem., Int. Ed.*, 2017, **56**, 2440–2444.

14 For the formation of N-TMS adducts of amides, see: (*a*) Y. Nagao, S. Miyamoto, M. Miyamoto, H. Takeshige, K. Hayashi, S. Sano, M. Shiro, K. Yamaguchi and Y. Sei, *J. Am. Chem. Soc.*, 2006, **128**, 9722–9729; (*b*) S. W. Djuric, *J. Org. Chem.*, 1984, **49**, 1311–1312. For preparation of silicon enolates from lithium amide enolates, see: (*c*) U. Frick and G. Simchen, *Liebigs Ann. Chem.*, 1987, **1987**, 839–845; (*d*) R. P. Woodbury and M. W. Rathke, *J. Org. Chem.*, 1978, **43**, 881–884. For the stability and C–H acidity of amide enolates, see: (*e*) J. P. Richard, G. Williams, A. C. O'Donoghu and T. L. Amyes, *J. Am. Chem. Soc.*, 2002, **124**, 2957–2968, and references therein; For a report on the effect of electrostatics on amide enolate stability, see: (*f*) P. R. Rablen and K. H. Bentrup, *J. Am. Chem. Soc.*, 2003, **125**, 2142–2147.

15 For selected examples of 7-aza-indoline Mannich donors, see: (*a*) F. A. Arteaga, Z. Liu, L. Brewitz, J. Chen, B. Sun, N. Kumagai and M. Shibasaki, *Org. Lett.*, 2016, **18**, 2391–2394; (*b*) L. Brewitz, F. A. Arteaga, L. Yin, K. Alagiri, N. Kumagai and M. Shibasaki, *J. Am. Chem. Soc.*, 2015, **137**, 15929–15939; (*c*) B. Sun, P. V. Balaji, N. Kumagai and M. Shibasaki, *J. Am. Chem. Soc.*, 2017, **139**, 8295–8301; (*d*) L. Yin, L. Brewitz, N. Kumagai and M. Shibasaki, *J. Am. Chem. Soc.*, 2014, **136**, 17958–17961. For select examples of N-acylpyrazoles, see: (*e*) J. Lu, Y. Fan, F. Sha, Q. Li and X.-Y. Wu, *Org. Chem. Front.*, 2019, **6**, 2687–2691.

16 S. Kobayashi, H. Kiyohara and M. Yamaguchi, *J. Am. Chem. Soc.*, 2011, **133**, 708–711.

17 Y. Yamashita, A. Noguchi, S. Fushimi, M. Hatanaka and S. Kobayashi, *J. Am. Chem. Soc.*, 2021, **143**, 5598–5604.

18 For a brief review of pyrrolidines in natural products, see: (*a*) D. O'Hagan, *Nat. Prod. Rep.*, 2000, **17**, 435–446; (*b*) C. Bhat and S. G. Tilve, *RSC Adv.*, 2014, **4**, 5405–5452.

19 For the synthesis of *N*-silyl imines *via* Aza-Peterson olefination, see: (*a*) G. Cainelli, D. Giacomini, M. Panunzio, G. Martelli and G. Spunta, *Tetrahedron Lett.*, 1987, **28**, 5369–5372; (*b*) D. J. Hart, K. Kanai, D. G. Thomas and T. K. Yang, *J. Org. Chem.*, 1983, **48**, 289–294.

20 N-TMS aryl imines have a boiling points of >60 °C at <0.5 mmHg and can be very challenging to distill when substitution on the arene is introduced. For examples of the synthesis and direct utilization of N-TMS imines, see: (*a*) J. M. Fernández-García, M. Á. Fernández-Rodríguez and E. Aguilar, *Org. Lett.*, 2011, **13**, 5172–5175; (*b*) J. Kikuchi, H. Ye and M. Terada, *Org. Lett.*, 2020, **22**, 8957–8961; (*c*) P. V. Ramachandran and T. E. Burghardt, *Chem.–Eur. J.*, 2005, **11**, 4387–4395; (*d*) D. A. Candito and M. Lautens, *Angew. Chem., Int. Ed.*, 2009, **48**, 6713–6716; (*e*) J. Vidal, S. Damestoy, L. Guy, J.-C. Hannachi, A. Aubry, A. Collet and A. Aubry, *Chem. Eur.*, 1997, **3**, 1691–1709; (*f*) S. E. Denmark, X. Su, Y. Nishigaichi, D. M. Coe, K.-T. Wong, S. B. D. Winter and J. Y. Choi, *J. Org. Chem.*, 1999, **64**, 1958–1967.

21 N. Gandhamsetty, J. Jeong, J. Park, S. Park and S. Chang, *J. Org. Chem.*, 2015, **80**, 7281–7287.

22 The assignment of Mannich product 4i is tentative based on the computational transition states elucidated for 4a and the diastereoselectivity of 4j & 4w determined *via* X-ray diffraction (see Schemes S1 and S2† for details). Due to A1,3 strain in the corresponding enolate of lactam 2i enolate, the beta-C-H bond in TS4 is expected to be syn-periplanar with the enolate oxygen in its most stable conformation. This conformation governs the approach of the imine electrophile from the methyl face due to the greater steric interaction present in the opposite facial approach. This selectivity is comparable to the result obtained for Mannich product 4J in which the backbone γ-methyl group favors the imine to approach from the opposite face, resuting in the major diastereomer 4j observed *via* XRD

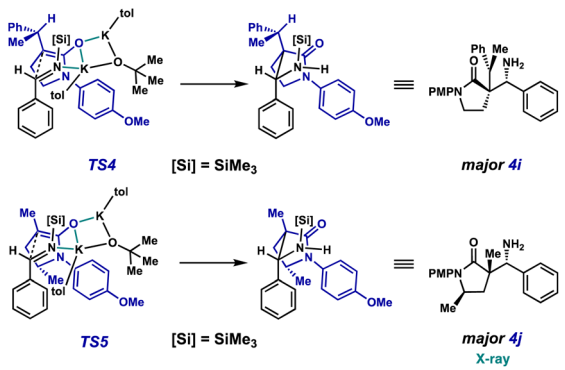

23 We observed the presence of Lewis basic heteroatoms significantly hindered the B(C6F5)3 catalyzed hydrosilylation. Esters, ketones, alkynes and nitro-groups were shown to be tolerant in a Ru-catalyzed hydrosilylation in D. V. Gutsulyak and G. I. Nikonov, *Angew. Chem., Int. Ed.*, 2010, **49**, 7553–7556.

24 V. Belot, D. Farran, M. Jean, M. Albalat, N. Vanthuyne and C. Roussel, *J. Org. Chem.*, 2017, **82**, 10188–10200.

25 C. Hansch, A. Leo and R. W. Taft, *Chem. Rev.*, 1991, **91**, 165–195.

26 For a mechanistic insight on the $B(C_6F_5)_3$-catalyzed hydrosilylation, see: (*a*) D. J. Parks, J. M. Blackwell and W. E. Piers, *J. Org. Chem.*, 2000, **65**, 3090–3098; (*b*) D. J. Parks and W. E. Piers, *J. Am. Chem. Soc.*, 1996, **118**, 9440–9441; (*c*) J. Hermeke, M. Mewald and M. Oestreich, *J. Am. Chem. Soc.*, 2013, **135**, 17537–17546; (*d*) J. M. Blackwell, E. R. Sonmor, T. Scoccitti and W. E. Piers, *Org. Lett.*, 2000, **2**, 3921–3923.

27 For examples of an RCM reaction of acrylamides to form an ε-lactam, see: (*a*) S. Fustero, F. Mojarrad, M. D. P. Carrión, J. F. Sanz-Cervera and J. L. Aceña, *Eur. J. Org Chem.*, 2009, **2009**, 5208–5214; (*b*) B. Sundararaju, T. Sridhar, M. Achard, G. V. M. Sharma and C. Bruneau, *Eur. J. Org Chem.*, 2010, **2010**, 6092–6096.

28 For a Pd-catalyzed, tandem *N*-arylation/carboamination sequence, see: (*a*) Q. Yang, J. E. Ney and J. P. Wolfe, *Org. Lett.*, 2005, **7**, 2575–2578; (*b*) J. E. Ney and J. P. Wolfe, *J.*

Am. Chem. Soc., 2005, **127**, 8644–8651; (*c*) G. S. Lemen and J. P. Wolfe, *Org. Lett.*, 2011, **13**, 3218–3221; (*d*) M. B. Bertrand, M. L. Leathen and J. P. Wolfe, *Org. Lett.*, 2007, **9**, 457–460.

29 For intramolecular Buchwald-Hartwig type annulations to form *N*-heterocycles, see: (*a*) J. A. Sirvent, F. Foubelo and M. Yus, *J. Org. Chem.*, 2014, **79**, 1356–1367; (*b*) L. Ding, J. Chen, Y. Hu, J. Xu, X. Gong, D. Xu, B. Zhao and H. Li, *Org. Lett.*, 2014, **16**, 720–723; (*c*) G. T. Notte and J. L. Leighton, *J. Am. Chem. Soc.*, 2008, **130**, 6676–6677.

30 The trans-diastereomer of tetrahydroquinoline 17 was observed to spontaneously oxidize to dihydroquinoline **18** when dissolved in $CDCl_3$.

31 Due to the low acidity of the amide α-C–H bond, we believe that lower base loadings result in too low of an initial concentration of potassium enolate **2'** to begin the catalytic cycle.

32 For computational studies of KOt-Bu tetramer-mediated reactions, see: (*a*) W.-B. Liu, D. P. Schuman, Y.-F. Yang, A. A. Toutov, Y. Liang, H. F. T. Klare, N. Nesnas, M. Oestreich, D. G. Blackmond, S. C. Virgil, S. Banerjee, R. N. Zare, R. H. Grubbs, K. N. Houk and B. M. Stoltz, *J. Am. Chem. Soc.*, 2017, **139**, 6867–6879; (*b*) Y. Lu, R. Zhao, J. Guo, Z. Liu, W. Menberu and Z.-X. Wang, *Chem.–Eur. J.*, 2019, **25**, 3939–3949; (*c*) I. D. Jenkins and E. H. Krenske, *ACS Omega*, 2020, **5**, 7053–7058.

33 DFT calculations were carried out at the M06-2X/6-311G++(d,p)/SMD(toluene)//M06-2X/6-31G(d) level of theory. Conformational sampling was performed using CREST. See SI for computational details.

34 For a recent computational study of stereoselective Mannich reactions, see: M. Feng, I. Mosiagin, D. Kaiser, B. Maryasin and N. Maulide, *J. Am. Chem. Soc.*, 2022, **144**, 13044–13049.

35 T. X. Gentner and R. E. Mulvey, *Angew. Chem., Int. Ed.*, 2021, **60**, 9247–9262.

36 Y.-F. Liu, L. Zheng, D.-D. Zhai, X.-Y. Zhang and B.-T. Guan, *Org. Lett.*, 2019, **21**, 5351–5356.

37 (*a*) D. A. Dougherty, *Acc. Chem. Res.*, 2013, **46**, 885–893; (*b*) Z.-W. Qu, H. Zhu, R. Streubel and S. Grimme, *ACS Catal.*, 2023, **13**, 1686–1692.